Surface restructuring, kinetic oscillations, and chaos in heterogeneous catalytic reactions

V. P. Zhdanov
Department of Applied Physics, Chalmers University of Technology, S-412 96 Göteborg, Sweden
and Boreskov Institute of Catalysis, Russian Academy of Sciences, Novosibirsk 630090, Russia
(Received 5 October 1998)

We present comprehensive Monte Carlo simulations of isothermal kinetic oscillations and chaos in catalytic reactions accompanied by adsorbate-induced surface restructuring. Our analysis is based on the lattice-gas model describing surface restructuring in terms of the statistical theory of first-order phase transitions. As an example, we treat the kinetics of the NO-H_2 reaction on the Pt(100) surface. A proposed reduced mechanism of this reaction includes NO adsorption, desorption, and decomposition occurring on the restructured patches of the surface (the decomposition products are rapidly removed from the surface via N_2 desorption and H_2O formation and desorption). Calculations are performed with a qualitatively realistic ratio between the rates of different elementary steps. In particular, NO diffusion is several orders of magnitude faster compared to the other steps. On the nm scale, the model predicts formation of restructured islands with atomically sharp boundaries. The shape of the islands is found to change dramatically with varying reaction conditions. Despite phase separation on the surface, the transition from almost harmonic oscillations (with relatively small separate islands) to chaos (with merging islands) is demonstrated to occur via the standard Feigenbaum scenario. Near the critical point, the dependence of the amplitude of oscillations on the governing parameter is shown to be close to that predicted for the Hopf supercritical bifurcation. [S1063-651X(99)10905-X]

PACS number(s): 05.45.−a, 05.50.+q, 68.35.Rh, 82.20.Wt

I. INTRODUCTION

Kinetic oscillations, observed in catalytic reactions on single-crystal surfaces at UHV conditions, often result from the interplay between reaction steps and adsorbate-induced surface restructuring [1,2] (nonisothermal effects are negligible at low pressures [1]). A classical example is CO oxidation on Pt(100) [3]. In this case, the (1×1) arrangement of metal atoms on the clean surface is metastable compared to a close packed quasihexagonal (''hex'') arrangement. CO adsorption may, however, stabilize the (1×1) phase. The latter provides a necessary (for oscillations) feedback between CO and oxygen adsorption because the rate of oxygen adsorption on the (1×1) patches is much higher than on the ''hex'' patches. Other examples include such reactions as CO+NO, NO+H_2, and NO+NH_3 on Pt(100).

The theoretical studies of kinetic oscillations accompa-

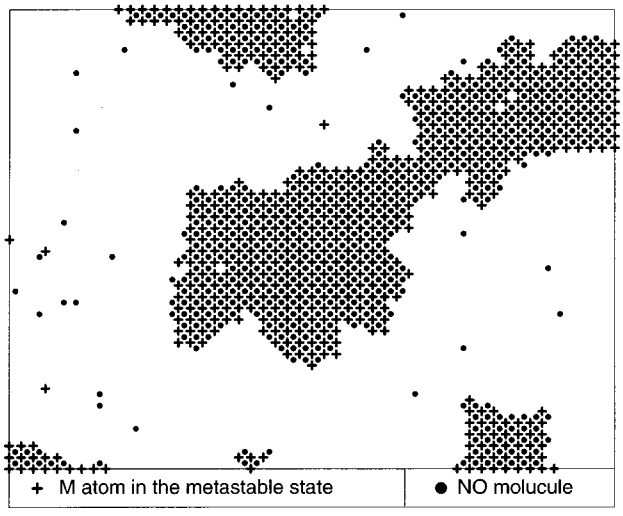

FIG. 1. Schematic arrangement of particles on the (40×50) lattice. Filled circles and plus signs exhibit adsorbed particles and substrate atoms in the metastable state, respectively. Metal atoms in the stable state are not shown.

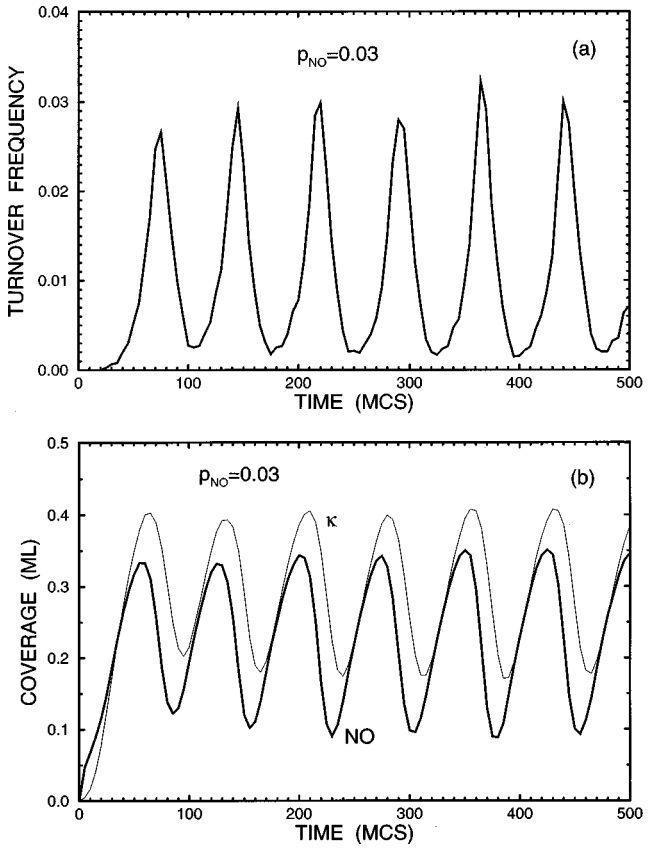

FIG. 2. (a) NO decomposition rate (per site per MCS) and (b) NO coverage and fraction κ of Pt atoms in the metastable state as a function of time for $p_{NO}=0.03$, $N_{diff}=1000$, and $L=200$.

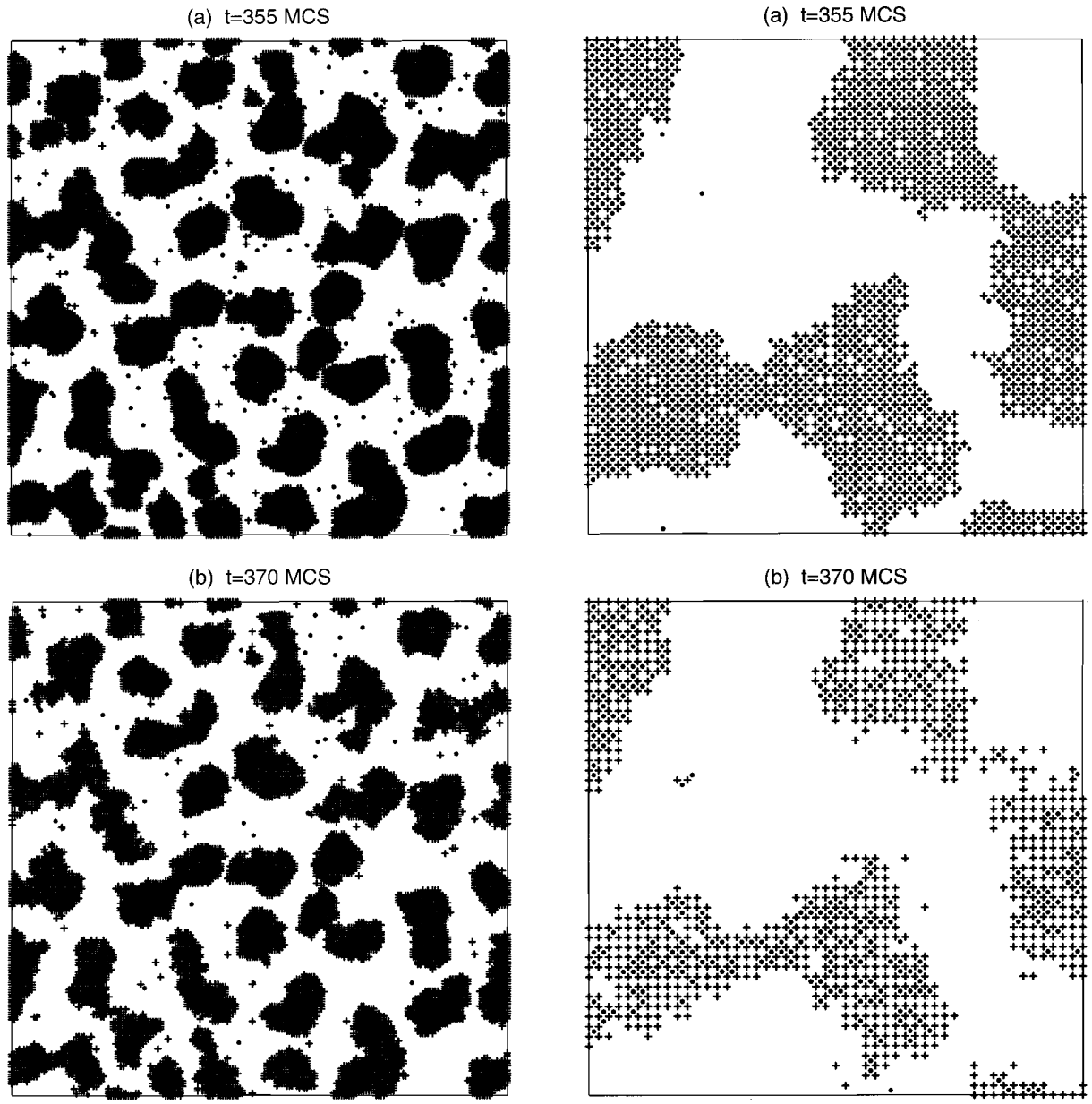

FIG. 3. Snapshots of a (200×200) lattice for the run, shown in Fig. 2, at five sequential stages when the fraction of Pt atoms in the metastable state is (a) maximum, (b) between maximum and minimum, (c) minimum, (d) between minimum and maximum, and (e) again maximum. The left panels show the whole lattice. The right panels, representing a (50×50) fragment of the lattice, exhibit the structure of the restructured islands in detail. The designations are as in Fig. 1.

nied by surface restructuring have primarily been aimed at CO oxidation on Pt. The treatments employing the mean-field (MF) kinetic equations [1,2] and Monte Carlo (MC) technique [4,5] were quite successful in reproducing the evolution of reactant coverages and reaction rate observed during oscillations. The MF models cannot, however, be used to analyze spatiotemporal distribution of adsorbed reactants on the nm scale because they operate only with average coverages of surface phases. In MC simulations, the distribution of adsorbed species can be calculated, but there exists another shortcoming connected with describing the adsorbate-induced changes in the surface. In all the available MC models [4,5], the pure mathematical rules employed to realize the steps related to surface restructuring are far from those prescribed by statistical mechanics. For example, surface diffusion of CO molecules is neglected or considered to be independent of the state of metal atoms. With such prescriptions, well-developed phases with atomically sharp phase boundaries, that are possible, are lacking, e.g., CO molecules are not able to induce the formation of (1×1) islands at relatively low coverages, because there is no driving force for phase separation. In contrast, experiments indicate that such islands are formed during CO adsorption on Pt(100) already at $\theta_{CO}\simeq0.08\pm0.05$ monolayer (ML) for $T\simeq500$ K [6] or even at $\theta_{CO}\simeq0.01$ ML for $T\simeq400$ K [7]. There are also direct observations of phase separation on the nm scale during kinetic oscillations in such reactions, e.g., as H_2 and CO oxidation occurring on a Pt(100) tip of a field ion microscope [8,9]. All these findings mean that the adsorbate-induced restructuring of the (100) face of Pt should be described in terms of the theory of first-order phase transitions. Meanwhile, the mathematical rules used in the available MC simu-

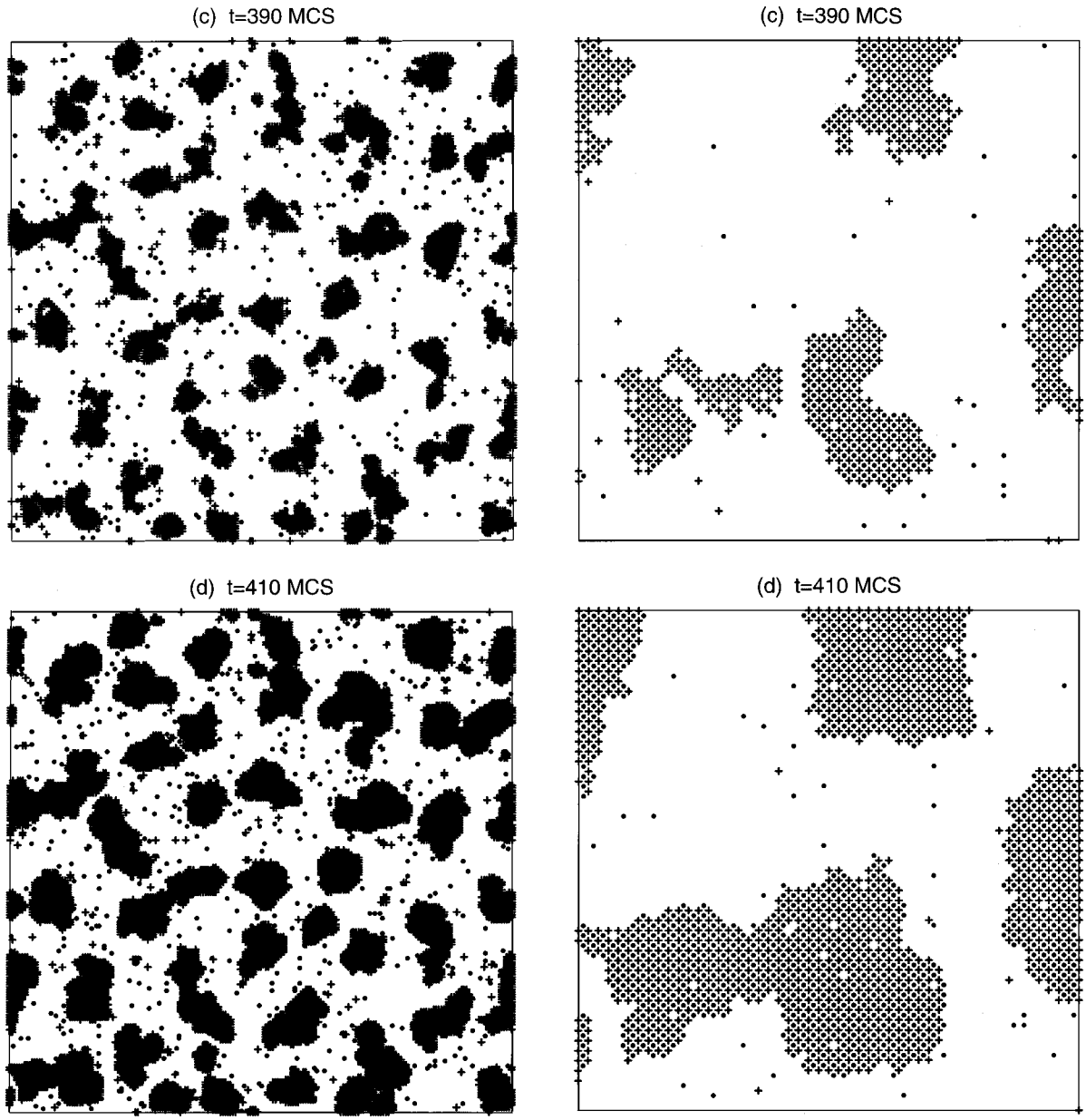

FIG. 3 (*Continued*).

lations have nothing in common with this theory.

Accurate description of adsorbate-induced surface restructuring on the basis of statistical theory of phase transitions is rather difficult because the understanding of microscopic details of this phenomenon is far from complete. Under such circumstances, it seems reasonable to formulate a simple well-defined lattice-gas model treating surface restructuring as a first-order phase transition and to employ this model for analyzing oscillatory kinetics. This approach was partially realized in our recent paper [10] where we proposed such a model and used it to analyze the influence of adsorbate-induced surface changes on thermal desorption spectra and propagation of chemical waves in bistable reactions. In the present paper, the same model is employed to treat kinetic oscillations in the NO-H_2 reaction on Pt(100). In principle, the model can be used to simulate other reactions (e.g., CO oxidation or NO reduction on Pt(100) [11]) as well. The analysis of the kinetics of the NO-H_2 reaction is, however, especially interesting, because a reduced mechanism of this reaction is fairly simple. For this generic mechanism, oscillations are predicted in a rather wide range of governing parameters. The latter makes it possible to simulate in detail various aspects of oscillatory kinetics. In particular, we show how oscillations arise and demonstrate the transition from regular oscillations to chaos. The kinetic curves are complemented by snapshots illustrating in detail the phase separation on the nm scale. A short preliminary report about the simulations presented was submitted elsewhere [12].

II. COMMENTS ON THE NO-H_2 REACTION ON PT(100)

Kinetic oscillations in the NO-H_2 reaction on Pt(100) were first observed by Nieuwenhuys and co-workers [13,14] at $P_{NO}=3\times10^{-9}$ bar, $P_{H_2}=(3-10)\times10^{-9}$ bar, and $T=420-520$ K. Later on, this phenomena was studied by Ertl and co-workers [15] at $P_{NO}=1.1\times10^{-9}$ bar, $P_{H_2}=$

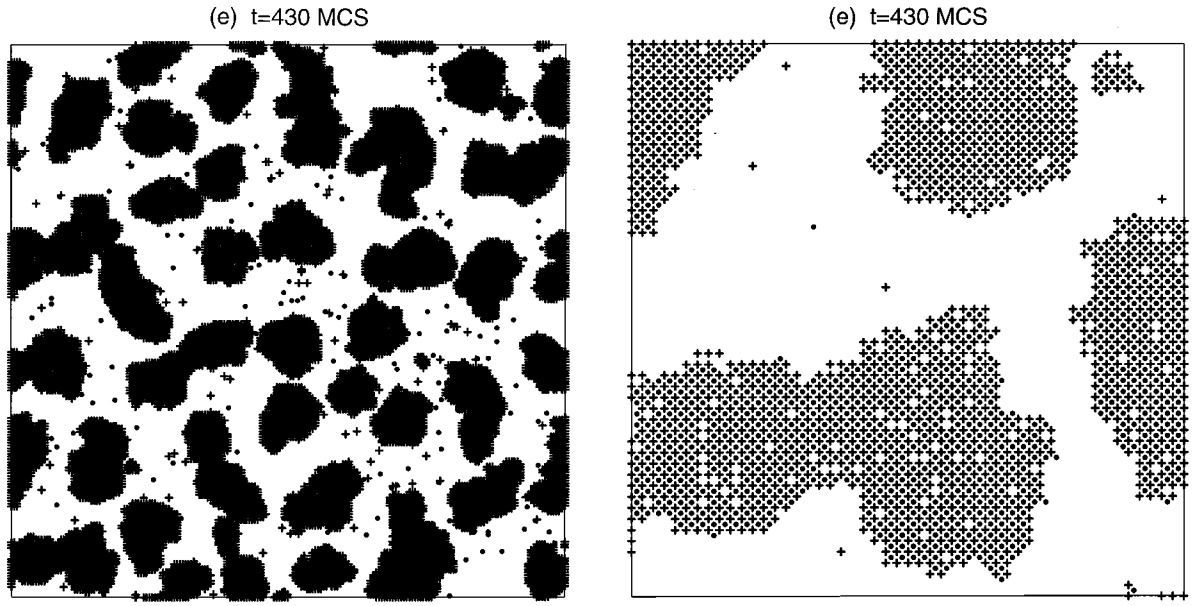

FIG. 3 (*Continued*).

3-10$\times 10^{-9}$ bar, and $T=430$-455 K. The latter group combined kinetic data with work function and low-energy electron diffraction (LEED) measurements. The temperature region in which oscillations were observed was found to coincide with the lifting of the ''hex'' reconstruction.

MF simulations of kinetic oscillations in the NO-H_2 reaction on Pt(100) were performed by Lombardo *et al.* [16], Gruyters *et al.* [17], and more recently by Makeev and Nieuwenhuys [18]. In the two former studies, surface restructuring was assumed to play a key role in oscillations. In contrast, Makeev and Nieuwenhuys are of the opinion that the oscillations result from the steps, which are not directly connected with surface restructuring. From our point of view, surface restructuring resulting in phase separation should be taken into account (at least above 430 K) because the kinetic equations describing chemical reactions on islands in the two-phase system are quite different compared to those used in the MF approximation.

The conventional mechanism of the NO-H_2 reaction on Pt(100) is as follows (''gas'' and ''ads'' mark gas phase and adsorbed particles):

$$(H_2)_{gas} \rightleftharpoons 2H_{ads}, \tag{1}$$

$$NO_{gas} \rightleftharpoons NO_{ads}, \tag{2}$$

$$NO_{ads} \rightarrow N_{ads} + O_{ads}, \tag{3}$$

$$2N_{ads} \rightarrow (N_2)_{gas}, \tag{4}$$

$$2H_{ads} + O_{ads} \rightarrow (H_2O)_{gas}, \tag{5}$$

$$3H_{ads} + N_{ads} \rightarrow (NH_3)_{gas}, \tag{6}$$

$$NO_{ads} + N_{ads} \rightarrow (N_2O)_{gas}. \tag{7}$$

Steps (5) and (6) are here not elementary [e.g., the NH_3 formation (6) is usually assumed to occur via sequential addition of H_{ad} to N_{ad}].

In general, one needs to take into account all the above steps. Practically, however, the reaction scheme can be reduced for the following reasons. (i) Our attention will be focused on the reaction behavior at relatively high temperatures ($T \simeq 460$ K) where one can observe the transition from oscillations to chaos [14]. In this case, the rate of N_2O for-

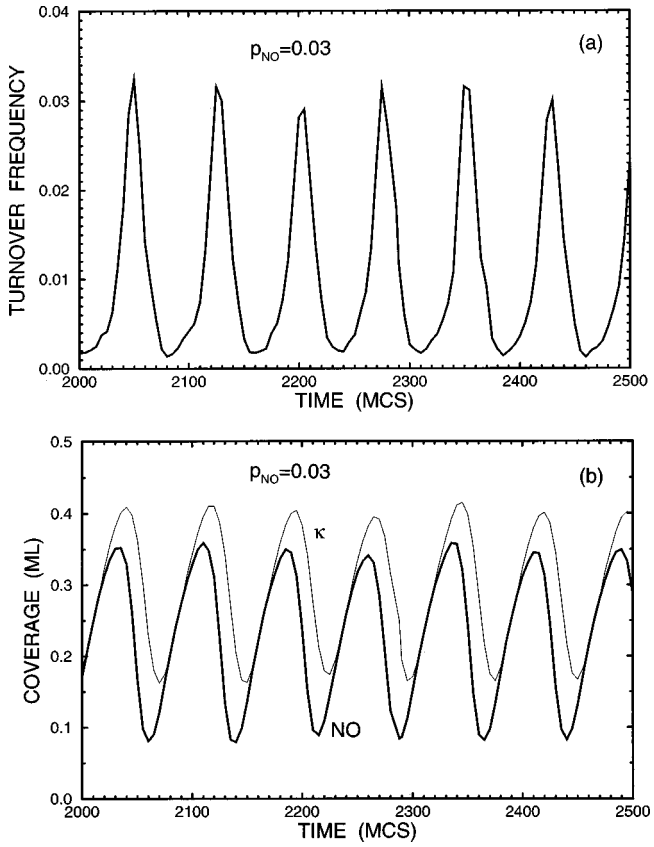

FIG. 4. (a) NO decomposition rate (per site per MCS) and (b) NO coverage and fraction of Pt atoms in the metastable state as a function of time for the same MC run as in Fig. 2, but at much later times.

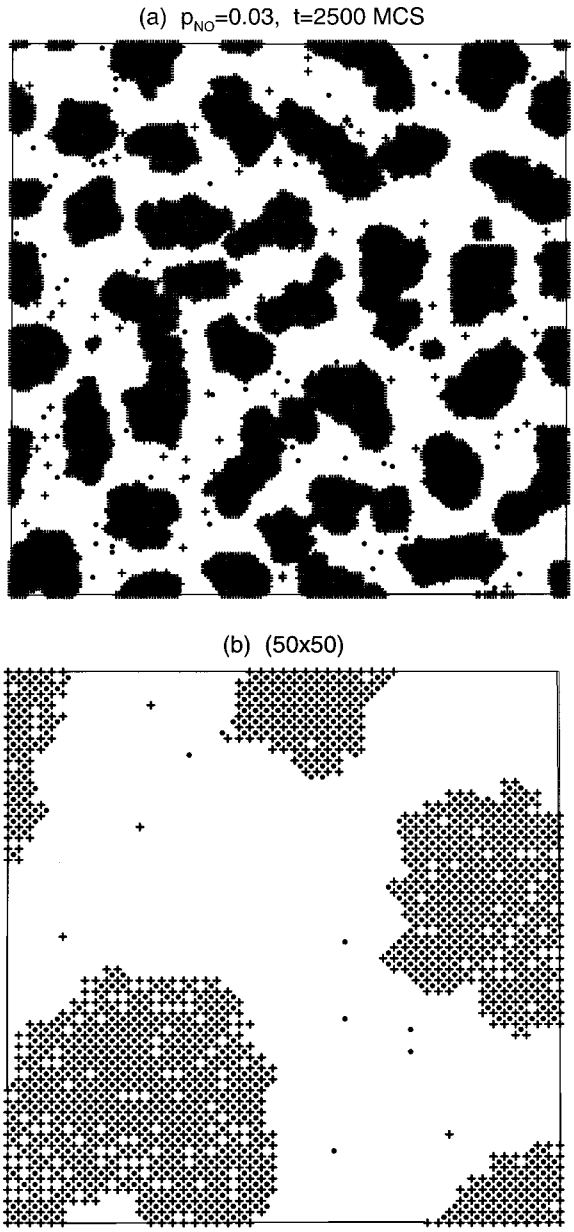

FIG. 5. Snapshots of a (200×200) lattice at the end of the run shown in Fig. 4. (a) The whole lattice and (b) a (50×50) fragment.

mation is relatively low [14] and accordingly step (7) can, as a first approximation, be omitted. (ii) Step (6) can be omitted as well because the rate of NH_3 formation is lower than that of N_2 desorption [14] provided that the H_2 pressure is not too high (in principle, the NH or NH_2 coverages might be appreciable, but such a scenario is not supported by the earlier simulations [16–18]). (iii) The steps resulting in H_2O formation are known to be very fast [19]. N_2 desorption is rather fast as well (the activation energy for this process is about 20 kcal/mol [16]). This means that the products of the NO decomposition [step (3)] can in simulations be simply removed from the surface just after successful decomposition trials. (iv) The main role of H_2 adsorption is to provide H atoms for step (5) (the effect of adsorbed hydrogen on surface restructuring is minor because the H coverage is low). But, removing O_{ad} just after NO decomposition, we do not need to analyze in detail step (5). In other words, we do not need to include H_2 adsorption explicitly.

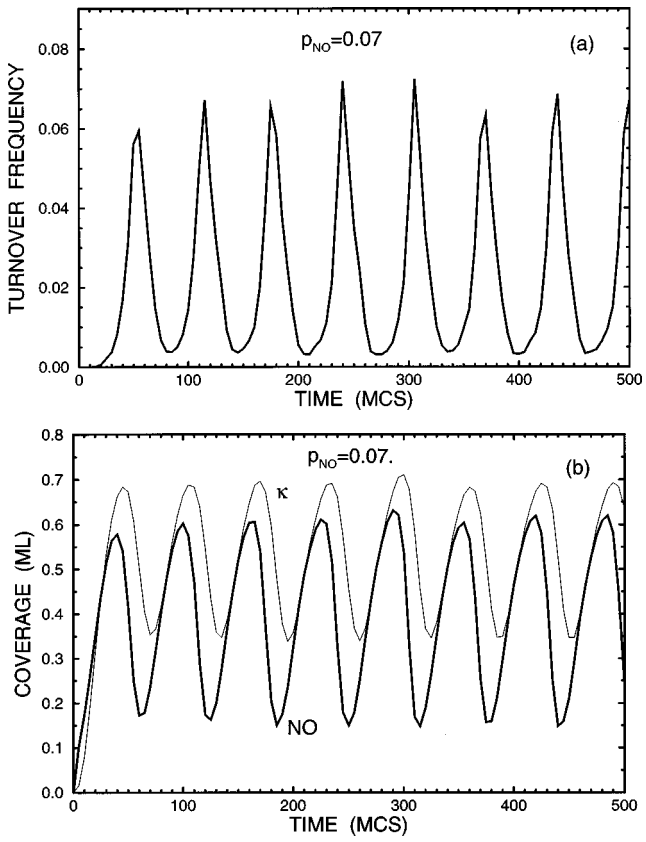

FIG. 6. As Fig. 2 for $p_{NO}=0.07$.

In summary, our reduced scheme of the NO-H_2 reaction on Pt(100) contains only two steps, namely, reversible NO adsorption (2) and decomposition (3). The decomposition products are removed from the surface immediately. Thus, we have only one adsorbed species, NO.

If one ignores NO-induced surface restructuring and assumes that all the adsorption sites are active in NO decomposition (as accepted in Ref. [18a]), the reduced reaction scheme is described in the MF approximation as

$$d\theta/dt = k_{ad}P_{NO}(1-\theta) - k_{des}\theta - k_{dec}\theta(1-\theta), \qquad (8)$$

where θ is the NO surface coverage (i.e., the average number of NO molecules per adsorption site), P_{NO} is the NO pressure, and k_{ad}, k_{des} and k_{dec} are adsorption, desorption and decomposition rate constants [the decomposition rate is proportional to $(1-\theta)$ because a NO molecule needs a vacant nearest-neighbor (NN) site for dissociation]. The unique steady-state solution of Eq. (8), $\theta = a - (a^2 - b)^{1/2}$[$a = (k_{ad}P_{NO} + k_{des} + k_{dec})/2k_{dec}$ and $b = k_{ad}P_{NO}/k_{dec}$], is stable (no oscillations). But in combination with surface restructuring, the model predicts oscillations and chaos.

III. MODEL

Adsorbate-induced surface restructuring results from lateral interactions between adsorbed particles, $A(A \equiv NO)$, and metal atoms, M. On Pt(100), the surface densities of M atoms in the stable and metastable structures are slightly different and the adsorbate-induced phase transition is then accompanied by ''forcing up'' some of the M atoms (the terms ''stable'' and ''metastable'' will hereafter always refer to the

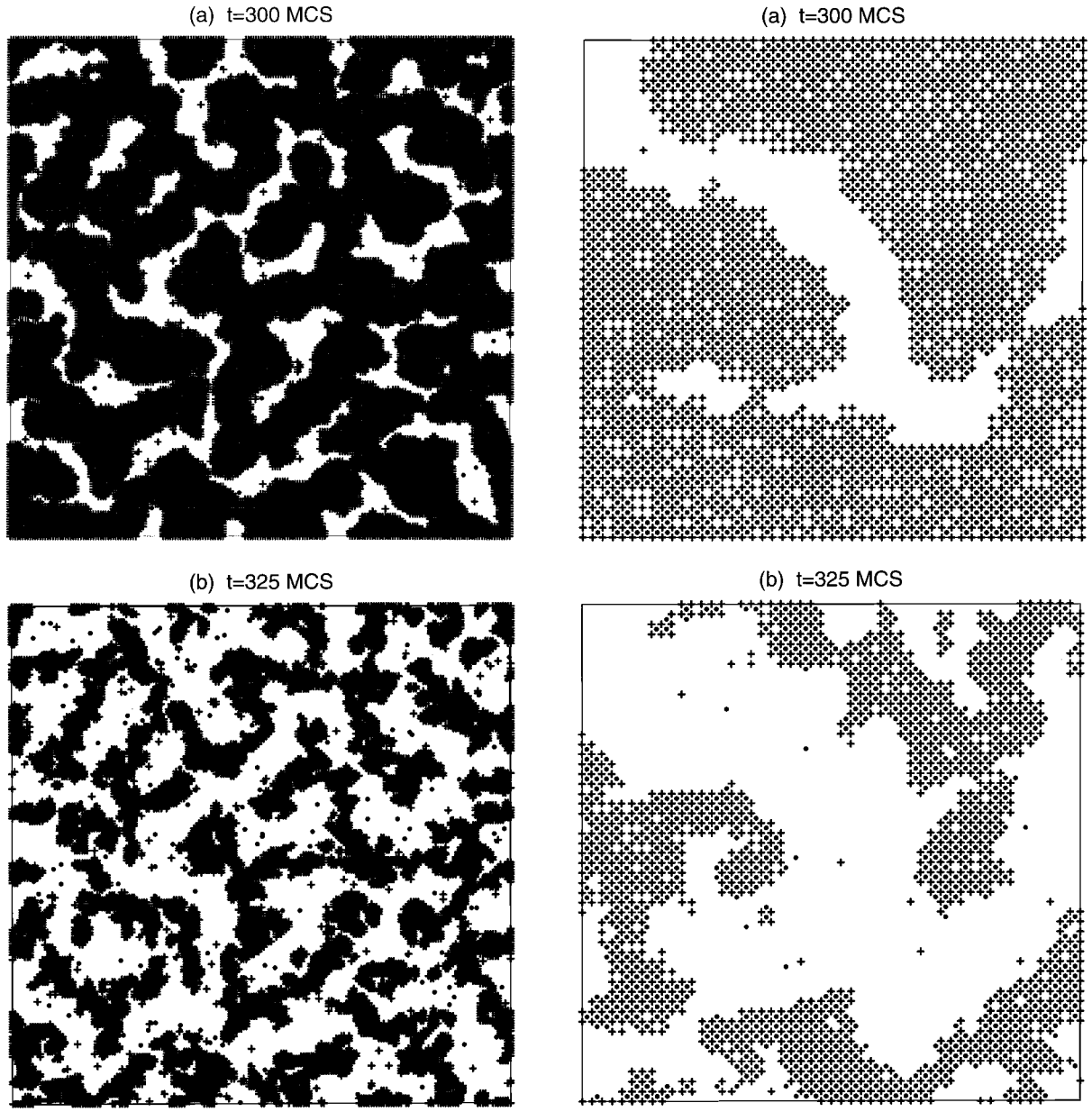

FIG. 7. Snapshots of a (200×200) lattice for the run, shown in Fig. 6, at three sequential stages when the fraction of Pt atoms in the metastable state is (a) maximum, (b) minimum, and (c) again maximum. The left and right panels show the whole lattice and a (50×50) fragment, respectively.

states that are stable and metastable on the *clean* surface). Full-scale simulations of the latter phenomenon are hardly possible at present. In our analysis, this complicating factor is ignored, i.e., the densities of M atoms in the stable and metastable structures are considered to be equal. In this case, the adsorbate-induced surface restructuring can be described by employing the lattice-gas model as shown in Fig. 1. The main ingredients of this model are as follows [10]:

(i) M atoms form a square lattice. Every M atom may be in the stable or metastable state. The energy difference of these states is ΔE. The NN M-M interaction is considered to be attractive, $-\epsilon_{MM}$ $(\epsilon_{MM}>0)$, if the atoms are in the same states, and repulsive, ϵ_{MM}, if the states are different (really, the total NN M-M interactions are of course attractive; the interactions $-\epsilon_{MM}$ and $+\epsilon_{MM}$ introduced describe the deviation from the average value). The next-nearest-neighbor interactions are ignored. With this choice of the M-M interactions, the model describes the tendency of substrate atoms to be either all in the stable or all in the metastable state.

(ii) Adsorbed particles occupy hollow sites (this assumption is not essential, because in the case of adsorption on top sites the structure of the formal equations will be the same). The adsorption energy of a given particle is considered to increase linearly with the number of NN substrate atoms in the metastable state (this is a driving force for the phase transition). In particular, the increase of the adsorption energy of an A particle after the transition of one NN substrate atom from the stable to the metastable state is ϵ_{AM} $(\epsilon_{AM}>0)$.

(iii) The NN adsorbate-adsorbate interaction is considered to be negligible or repulsive, $\epsilon_{AA}\geqslant0$.

The Hamiltonian corresponding to the assumptions above contains the substrate, adsorbate-substrate, and adsorbate-adsorbate interactions,

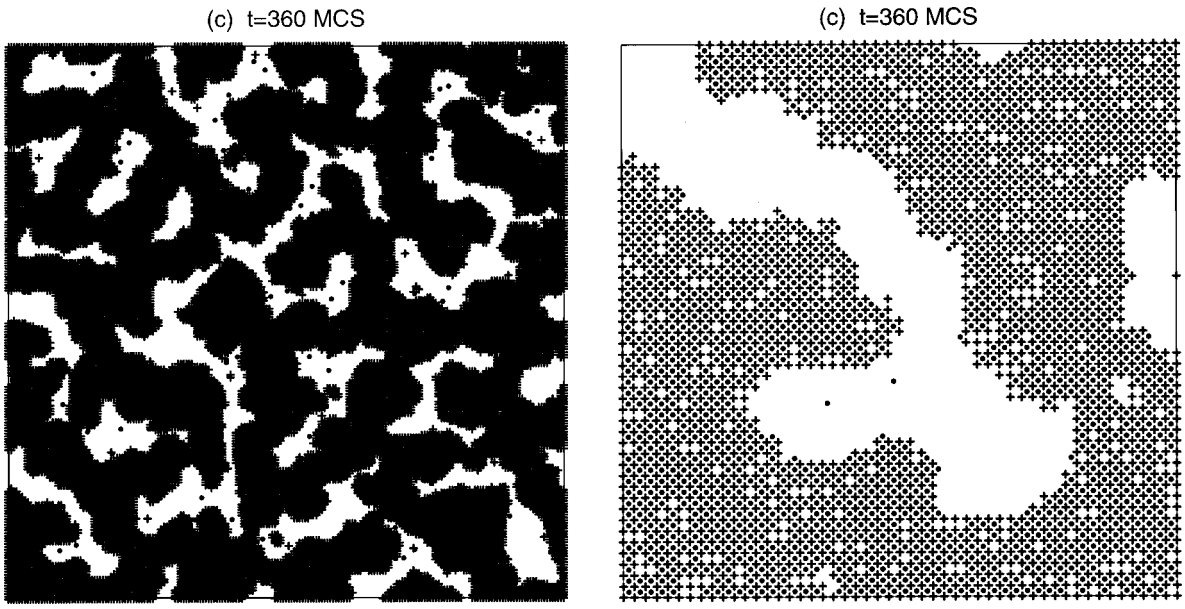

FIG. 7 (*Continued*).

$$H = H_s + H_{\rm as} + H_a , \tag{9}$$

$$H_s = \Delta E \sum_i n_i^M - 4\epsilon_{MM} \sum_{i,j} (n_i^M - 1/2)(n_j^M - 1/2), \tag{10}$$

$$H_{\rm as} = -\sum_{i,j} \epsilon_{AM} n_j^A n_i^M , \tag{11}$$

$$H_a = \sum_{i,j} \epsilon_{AA} n_i^A n_j^A , \tag{12}$$

where n_i^M is the variable characterizing the state of atom i ($n_i^M = 1$ or 0 is assigned to the metastable and stable states, respectively), n_i^A is the occupation number of the adsorption sites, and $\Sigma_{i,j}$ means summation over NN pairs.

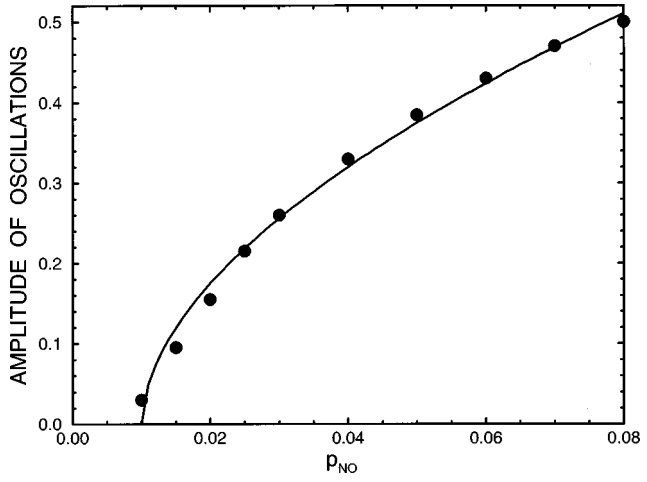

FIG. 8. Amplitude of period-1 oscillations of NO coverage as a function of $p_{\rm NO}$. Filled circles exhibit the MC data obtained with $N_{\rm diff} = 1000$ and $L = 200$ (the average statistical error in the results is shown by the size of the data points). The solid line corresponds to the power-law dependence, $\Delta\theta \propto (p_{\rm NO} - p_{\rm NO}^{\rm cr})^x$, with $p_{\rm NO}^{\rm cr} = 0.01$ and $x = 0.55$.

An elementary analysis [10] shows that the model outlined predicts an adsorbate-induced first-order phase transition provided that the adsorbate-substrate interaction is sufficiently strong. Thus, what we need in our simulations is to introduce the rate constants for all the relevant elementary rate processes in accordance with the model. General pre-

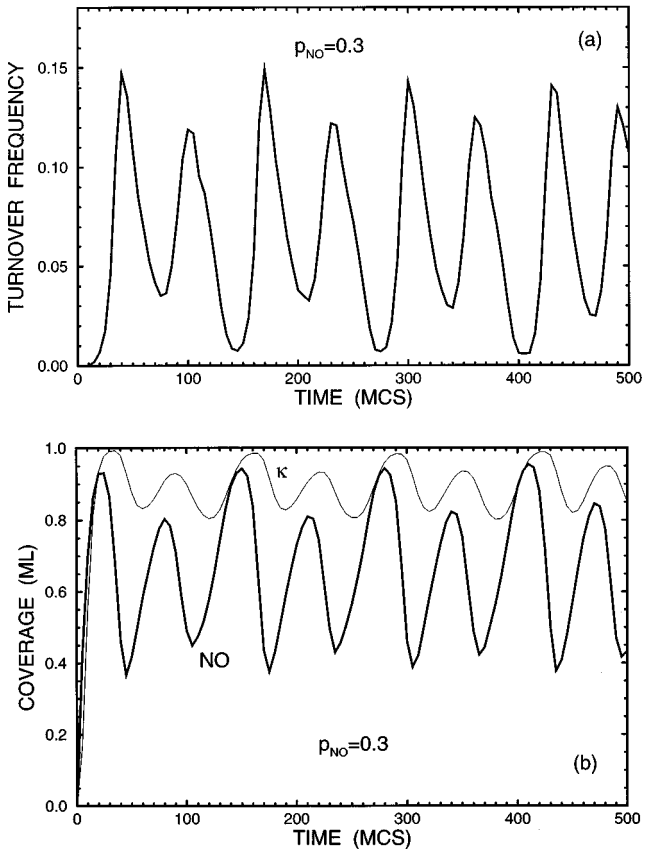

FIG. 9. (a) NO decomposition rate (per site per MCS) and (b) NO coverage and fraction of Pt atoms in the metastable state as a function of time for $p_{\rm NO} = 0.3$, $N_{\rm diff} = 1000$, and $L = 200$.

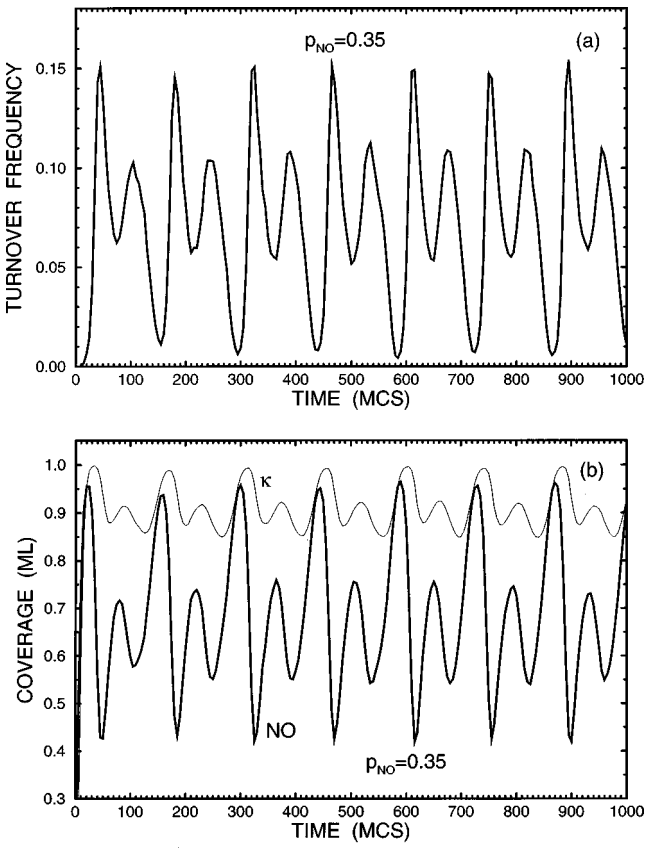

FIG. 10. As Fig. 9 for $p_{\mathrm{NO}}=0.35$.

scriptions how to realize this procedure are described in Ref. [20]. The simplest reasonable set of rules for simulating elementary reaction steps is as follows.

Adsorption of A particles occurs on vacant adsorption sites with unit probability.

Desorption of A particles is affected by A-A and A-M lateral interactions. The normalized dimensionless probability of desorption of a given particle is defined as (we use $k_{\mathrm{B}}=1$)

$$W_{\mathrm{des}}=\exp(\mathcal{E}_i/T), \tag{13}$$

where $\mathcal{E}_i=\Sigma_j(\epsilon_{AA}n_j^A-\epsilon_{AM}n_j^M)$ is a sum of NN interactions.

Diffusion of A particles occurs via jumps to NN vacant sites. The probabilities of these jumps usually depend [20] on lateral interactions in the ground and activated states (the terms ''activated'' and ''ground'' correspond here to the transition state theory). Taking into account that the details of diffusion complicated by adsorbate-substrate lateral interactions are not well established, we use for the jump probabilities the Metropolis (MP) rule, $W_{\mathrm{dif}}=1$ for $\Delta\mathcal{E}\leqslant 0$, and $W_{\mathrm{dif}}=\exp(-\Delta\mathcal{E}/T)$ for $\Delta\mathcal{E}>0$, where $\Delta\mathcal{E}$ is the energy difference between the final and initial states. This rule, compatible with the detailed balance principle, seems to be reasonable in our case (at least as a first approximation) because it predicts rather rapid diffusion on perfect stable or metastable patches, rapid jumps at the phase boundaries from the perfect to the metastable phase, but slow jumps in the opposite direction (because the adsorption energy on metastable patches is higher).

Decomposition of A (i.e., of NO) occurs provided that (a) at least one NN site is vacant and (b) all the M atoms adjacent to A and to a vacant site are in the metastable state [the latter condition takes into account that NO decomposition occurs primarily on the (1×1) phase [16]]. The effect of lateral interactions on the A-decomposition rate is for simplicity neglected (if necessary, it can be taken into account as described in Ref. [21]).

Surface restructuring occurs via changes of the state of M atoms. The probabilities of the transitions from the metastable to the stable state and back are given by the MP rule (as in the case of A diffusion).

Reaction steps and adsorbate-induced surface restructuring are accompanied by release of heat. At UHV conditions, the rate of heat generation is low and the heat disposal is fairly effective. Under such circumstances, the kinetic oscillations are practically isothermal [1]. For this reason, we in our simulations neglect the nonisothermal effects. The nonthermal effects (''hot'' atoms or molecules, etc.) are neglected as well, because the role of such effects in kinetic oscillations is expected to be minor (for a relevant discussion, see Sec. 2.3.3 in Ref. [20]).

IV. MODEL PARAMETERS

To simulate the reaction kinetics, we use the following set of parameters: $\Delta E/T=2$, $\epsilon_{MM}/T=0.5$, and $\epsilon_{AM}/T=2$ (such values are typical for surface restructuring). The A-A lateral interactions are for simplicity neglected, $\epsilon_{AA}=0$. For this set of the model parameters corresponding to fixed temperature, we have $T\simeq 0.40T_c$, where T_c is the critical temperature for the first-order adsorbate-induced phase transition on the surface (T_c was calculated by analyzing the A adsorption isotherms at different temperatures).

In addition, we need to introduce the dimensionless parameters, p_{res} and p_{rea} $(p_{\mathrm{res}}+p_{\mathrm{rea}}\leqslant 1)$, characterizing the relative rates of surface restructuring, adsorption-reaction steps, and diffusion of A particles. The rates of these processes are considered to be proportional to p_{res}, p_{rea}, and $1-p_{\mathrm{res}}-p_{\mathrm{rea}}$, respectively. In reality, the rate of surface restructuring is lower than that of the adsorption-reaction steps (i.e., $p_{\mathrm{res}}<p_{\mathrm{rea}}$), which are in turn much slower compared to A diffusion (i.e. $p_{\mathrm{res}}+p_{\mathrm{rea}}\ll 1$). In our simulations, we employ $p_{\mathrm{res}}/(p_{\mathrm{res}}+p_{\mathrm{rea}})=0.3$. In addition, we use the number $N_{\mathrm{dif}}\equiv(1-p_{\mathrm{res}}-p_{\mathrm{rea}})/(p_{\mathrm{res}}+p_{\mathrm{rea}})$ characterizing the ratio of the rates of A diffusion and the other processes. The results below are presented for $N_{\mathrm{dif}}=1000$.

In our model, the catalytic cycle includes A (NO) adsorption, desorption, and decomposition. To simulate these steps, we introduce the dimensionless parameters p_{NO} for A adsorption and p_{des} for A desorption. The rates of these processes are assumed to be proportional to p_{NO} and p_{des}, respectively. The A decomposition rate is considered to be proportional to $1-p_{\mathrm{des}}$. The simulations were executed for $p_{\mathrm{des}}=0.3$.

V. ALGORITHM OF SIMULATIONS

The MC algorithm for simulating the reaction kinetics consists of sequential trials of reaction, surface restructuring, and A diffusion. A random number ρ $(\rho\leqslant 1)$ is generated. If $\rho<p_{\mathrm{rea}}$, an adsorption-reaction trial is realized [item (a)].

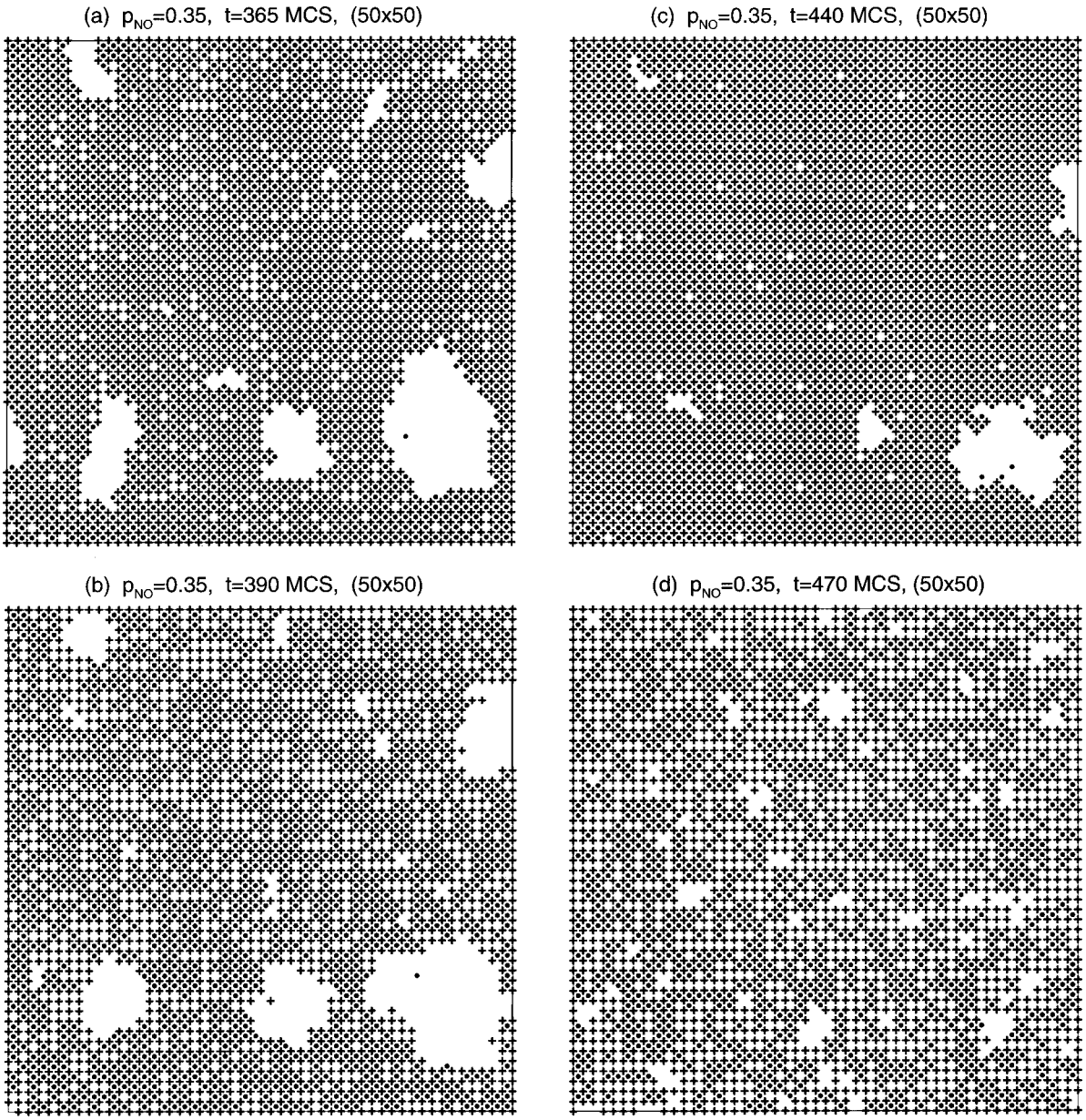

FIG. 11. Snapshots of a (200×200) lattice for the run, shown in Fig. 10, at four sequential stages when the NO coverage is (a) maximum, (b) minimum, (c) maximum, and (d) again minimum.

For $p_{\rm rea}<\rho<p_{\rm rea}+p_{\rm res}$, an attempt of surface restructuring is executed [item (b)]. If $\rho>p_{\rm rea}+p_{\rm res}$, an A-diffusion trial is performed [item (c)].

(a) An adsorption-reaction trial contains several steps. (i) An adsorption site is chosen at random. (ii) A new random number ρ' is generated. (iii) If the site selected is vacant, A adsorption is realized provided that $\rho'<p_{\rm NO}$. (iv) If the site selected is occupied by A, A desorption or decomposition is realized for $\rho'<p_{\rm des}$ and $\rho'>p_{\rm des}$, respectively. For A desorption, a new random number ρ'' is generated and the attempt is accepted if $\rho''<W_{\rm des}$, where $W_{\rm des}\leqslant1$ is the normalized desorption probability given by Eq. (13). For A decomposition, one of the NN sites is chosen at random and the trial is accepted if this site is vacant and adjacent M atoms are in the metastable state.

(b) For surface restructuring, a M atom selected at random tries to change its state according to the MP rule.

(c) For A diffusion, an adsorption site is chosen at random. If the site is vacant, the trial ends. Otherwise, an A particle located in this site tries to diffuse. In particular, an adjacent site is randomly selected, and if the latter site is vacant, the A particle jumps to it with the probability prescribed by the MP rule.

Simulating the reaction kinetics, we consider that initially (at $t=0$) the surface is clean and all the M atoms are in the stable state. The results have been obtained for $(L\times L)$ M lattices with $L=200$ and periodic boundary conditions. For oscillatory kinetics accompanied by phase separations, these boundary conditions make sense provided that the typical size of islands is much lower than the lattice size. The latter requirement is fulfilled in our study.

To measure time, we use the so-called MC step (MCS) defined as $(L\times L)$ attempts of the adsorption-reaction-surface-restructuring events. In principle, one might define

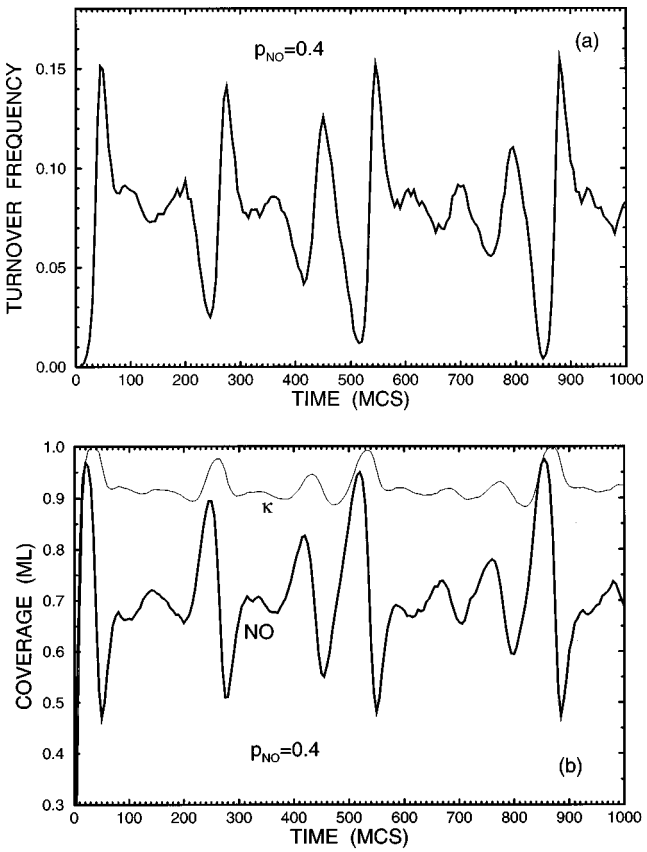

FIG. 12. As Fig. 9 for $p_{NO}=0.4$.

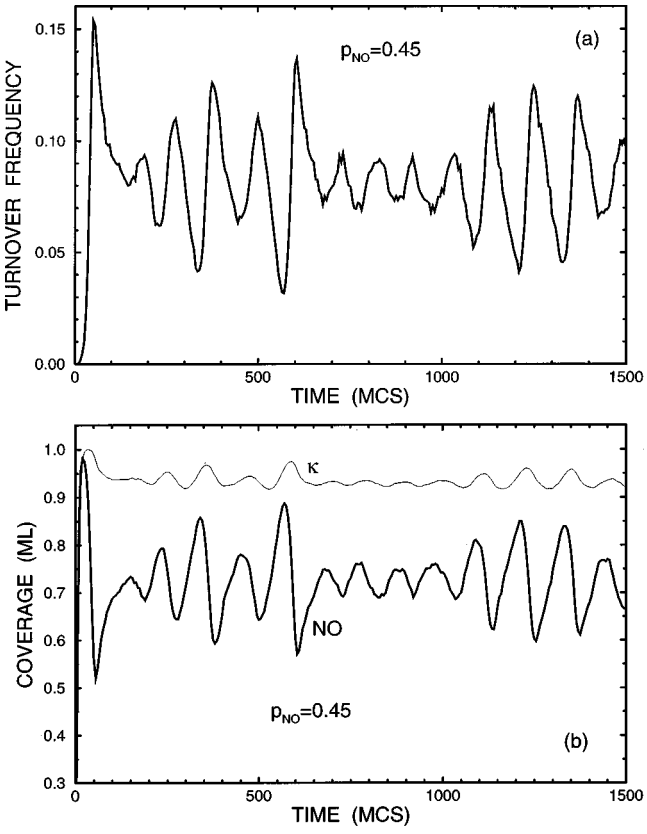

FIG. 13. As Fig. 9 for $p_{NO}=0.45$.

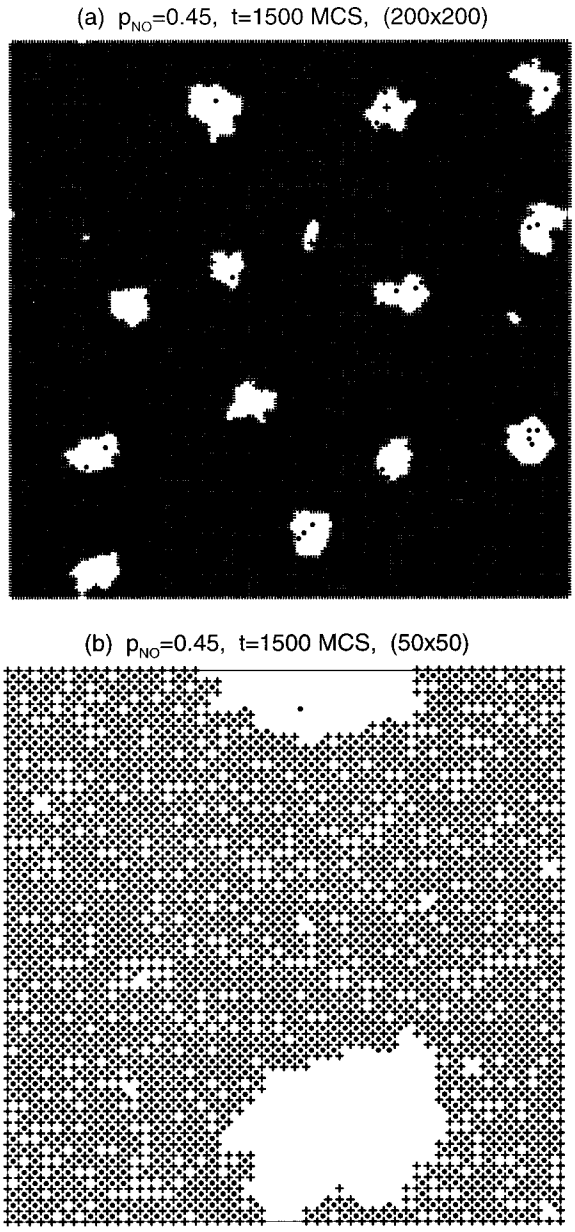

FIG. 14. Snapshots of a (200×200) lattice at the end of the run, shown in Fig. 13. (a) The whole lattice and (b) a (50×50) fragment.

one MCS as $(L\times L)$ trials of adsorption, reaction, A diffusion, and surface restructuring. In the latter case, the time scale would primarily be connected with A diffusion, because in our simulations this process is rapid compared to other steps. Our experience indicates, however, that the effect of diffusion on the period of oscillations is fairly weak (provided that the time scale is not directly related to the diffusion rate). Under such circumstances, it does not seem to be reasonable to choose the diffusion-based time scale.

Finally, it is worth discussing the relationship between the dimensionless MC probabilities and time and real rate constants and time. Describing the catalytic cycle, we have considered that the sum of the maximum probabilities of desorption and decomposition is equal to unity. Physically, this means that $p_{des}=k_{des}/(k_{des}+k_{dec})$ and $p_{dec}\equiv1-p_{des}=k_{dec}/(k_{des}+k_{dec})$, where k_{des} and k_{dec} are the maximum

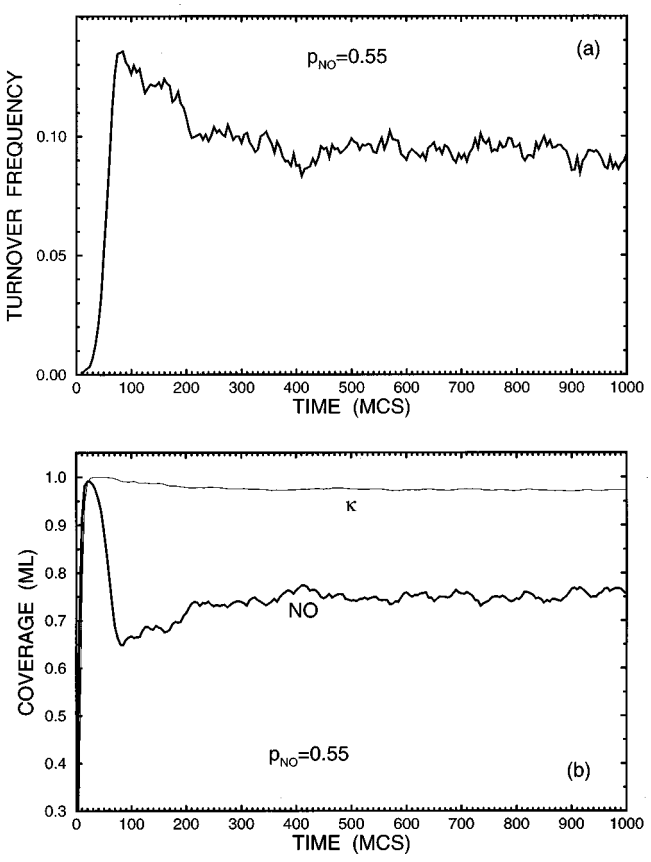

FIG. 15. As Fig. 9 for $p_{NO}=0.55$.

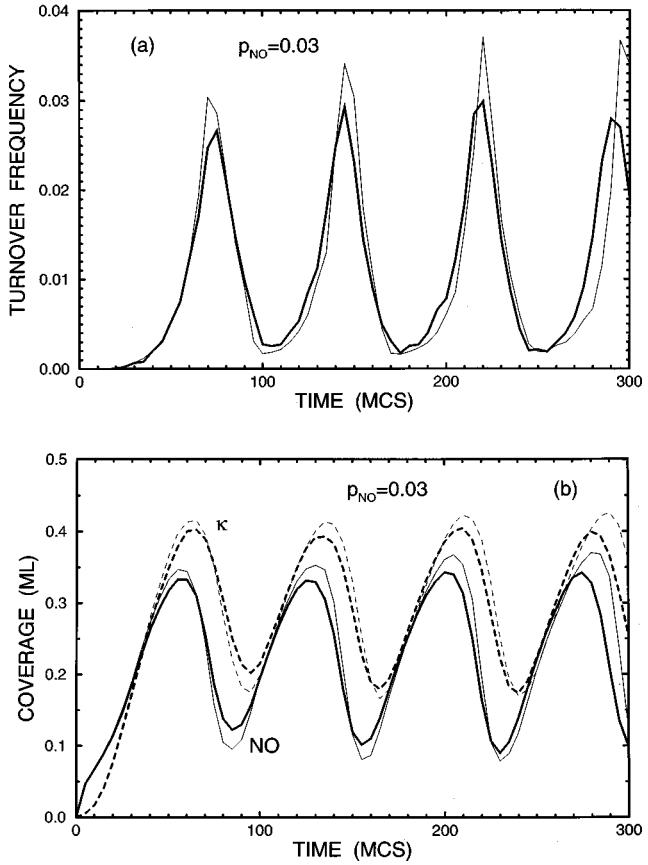

FIG. 16. (a) NO decomposition rate (per site per MCS) and (b) NO coverage and fraction of Pt atoms in the metastable state as a function of time for $p_{NO}=0.3$ and $L=200$. Thick and thin lines show the results for $N_{diff}=10^3$ and 10^4, respectively.

values of the desorption and decomposition rate constants. For A adsorption, we accordingly have $p_{NO}=k_{ad}P_{NO}/(k_{des}+k_{dec})$, where $k_{ad}P_{NO}$ is the rate (per site) of adsorption on a clean surface (k_{ad} is the adsorption rate constant, and P_{NO} is the NO pressure). The MC time is defined in our simulations via the adsorption-reaction-surface-restructuring events. This means that the MC and real times are interconnected as $t_{MC}=(k_{des}+k_{dec}+k_{res})t$ (k_{res} is the maximum value of the rate constant of surface restructuring).

VI. RESULTS OF SIMULATIONS

With the specification above (Sec. IV), we have only one governing parameter, p_{NO} (this parameter is proportional to NO pressure). Well-developed oscillatory kinetics are found for $0.01\leqslant p_{NO}\leqslant 0.5$. Physically, it is clear that oscillations can really be observed in such a broad interval only provided that the H_2 pressure is changed together with the NO pressure in order to guarantee applicability of the reduced model (the experiment [14] does show oscillations in a wide NO-pressure range provided that the ratio of NO and H_2 pressures is kept approximately constant).

With increasing p_{NO} from 0.01 to 0.5, the model predicts transition from almost harmonic oscillations to chaos via the standard Feigenbaum scenario [22]. Period-1 oscillations are observed at $0.01\leqslant p_{NO}<0.25$. Period-2 oscillations occur at $0.25\leqslant p_{NO}<0.25$. For $p_{NO}\simeq 0.4$, the kinetics look approximately like period-4 oscillations. At $0.4<p_{NO}<0.5$, we observed irregular (chaotic) oscillations.

A. Mechanism of period-1 oscillations

The mechanism of period-1 oscillations can be understood by analyzing the reaction kinetics in combination with spatiotemporal patterns. For example, let us consider the data (Fig. 2 and 3) for $p_{NO}=0.03$. In this case, the average NO coverage is relatively small, $\langle\theta\rangle\simeq 0.2$ (Fig. 2), and NO molecules form well-developed nonoverlapping mesoscopic islands with atomically sharp boundaries (Fig. 3). The first stage for analyzing sustained oscillations can be chosen arbitrarily. We start from the point when the fraction of Pt atoms in the metastable state is maximum [Fig. 3(a)]. In this case, the restructured islands are relatively large, the local NO coverage inside islands is rather high, and an additional supply of NO molecules to the islands from the unrestructured patches is almost perfectly balanced by NO decomposition inside islands. The balance is, however, not completely perfect because NO decomposition is an autocatalytic process. Thus, the NO coverage inside islands starts to decrease. The latter is accompanied by a slow decrease of the restructured islands and also by formation of defects in the island structure [Fig. 3(b)]. With increasing time, the restructured islands become rather small [Fig. 3(c)]. Supply of NO molecules to such islands from the unrestructured patches results in the increase of NO coverage inside islands. The latter stabilizes the island structure and the islands start to grow [Fig. 3(d)]. Eventually, the islands again become relatively large [Fig. 3(e)]. Comparing Figs. 3(a) and 3(e) shows that

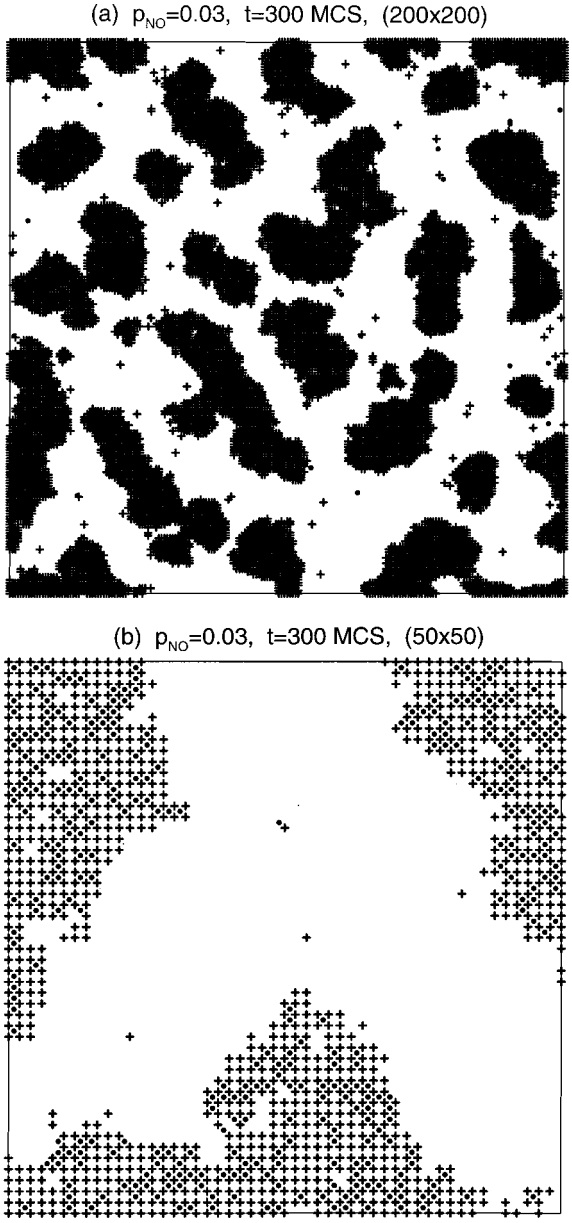

FIG. 17. Snapshots of a (200×200) lattice at the end of the run (with $N_{\rm diff}=10^4$), shown in Fig. 16 by the thin lines. (a) The whole lattice and (b) a (50×50) fragment.

the changes in the shape of islands during the oscillation period are visible but not dramatic.

The kinetics shown in Fig. 2 has been run up to $t=500$ MCS's. One might expect (in analogy with spinodal decomposition) that oscillations observed are accompanied with increasing time by slow growth of the average (over the oscillation period) island size and accordingly by slow increase (or decrease) of the oscillation period. Our simulations indicate, however, that this is not the case. For example, Fig. 4 exhibits the same MC run as in Fig. 2, but at much longer times (up to $t=2500$ MCS). Comparing Figs. 2 and 4 indicates that the period and amplitude of oscillations do not change with increasing time. The typical size of islands does not change either [cf. Figs. 2(a), 2(e), and 5, showing the lattice snapshots for the stage when the fraction of Pt atoms in the metastable state is maximum].

With increasing $p_{\rm NO}$ (see, e.g., Figs. 6 and 7 for $p_{\rm NO}=0.07$), the average NO coverage increases. The amplitude of oscillations increases as well, but the period of oscillations slightly decreases. The mechanism of oscillations remains basically the same, but the shape of islands becomes eventually quite different due to the merger of islands (Fig. 7).

B. Amplitude of period-1 oscillations vs. $p_{\rm NO}$

With changing a governing parameter p kinetic oscillations described by ordinary differential equations arise usually via the Hopf supercritical bifurcation [22]. According to this scenario, the amplitude of oscillations near the critical point is proportional to $(p-p_{\rm cr})^{1/2}$. There is, however, no, guarantee that the conventional arguments resulting in the square-root dependence are applicable in our case, because our model predicting phase separation can hardly be described by ordinary differential equations. For this reason, it was of interest to study in detail the kinetics of oscillations near $p_{\rm NO}^{\rm cr}$. Our analysis (Fig. 8) indicates that in this region the amplitude of oscillations of NO coverage is proportional to $(p_{\rm NO}-p_{\rm NO}^{\rm cr})^x$ with $x=0.55\pm0.05$. This finding is close to that predicted for the Hopf bifurcation.

C. Transition to chaos

For $p_{\rm NO}$ slightly above 0.25, we observed period-2 oscillations. Typical examples of such oscillations are presented for $p_{\rm NO}=0.3$ and 0.35 in Figs. 9 and 10, respectively. In the former case (Fig. 9), the shape of kinetic curves is close to that of period-1 oscillations. In the latter case (Fig. 10), period-2 oscillations are developed much better. Typical lattice snapshots for the run shown in Fig. 10 are exhibited in Fig. 11. Some of the features of these snapshots could be expected in advance. Comparing, for example, the surface structures corresponding to two sequential maximums of NO coverage [Figs. 11(a) and 11(c)], one can find that the restructured area is ordered much better and the size of spots formed by vacant sites is lower in the case of the maximum with a higher coverage value [Fig. 11(c)]. Despite such findings, it seems to be rather difficult to rationalize in detail (as it was done for period-1 oscillations) the mechanism of period-2 oscillations.

For $p_{\rm NO}=0.4$, the reaction kinetics look (Fig. 12) approximately like period-4 oscillations.

Irregular oscillations have been observed at $0.4<p_{\rm NO}<0.5$. An example of chaotic oscillations (for $p_{\rm NO}=0.45$) is shown in Fig. 13. The corresponding snapshots are exhibited in Fig 14.

With further increasing $p_{\rm NO}$, oscillations are lacking because the system is rapidly trapped to the state where the NO coverage is high and almost all the surface is restructured (see, e.g., Fig. 15 for $p_{\rm NO}=0.55$).

D. Role of diffusion, etc.

In heterogeneous catalytic reactions, diffusion of adsorbed species is usually fast compared to other steps. In the simulations above, NO diffusion was three orders of magnitude faster ($N_{\rm dif}=1000$) than NO adsorption and dissociation and surface restructuring. In reality, the difference of the rates of these steps is expected to be much higher. For this

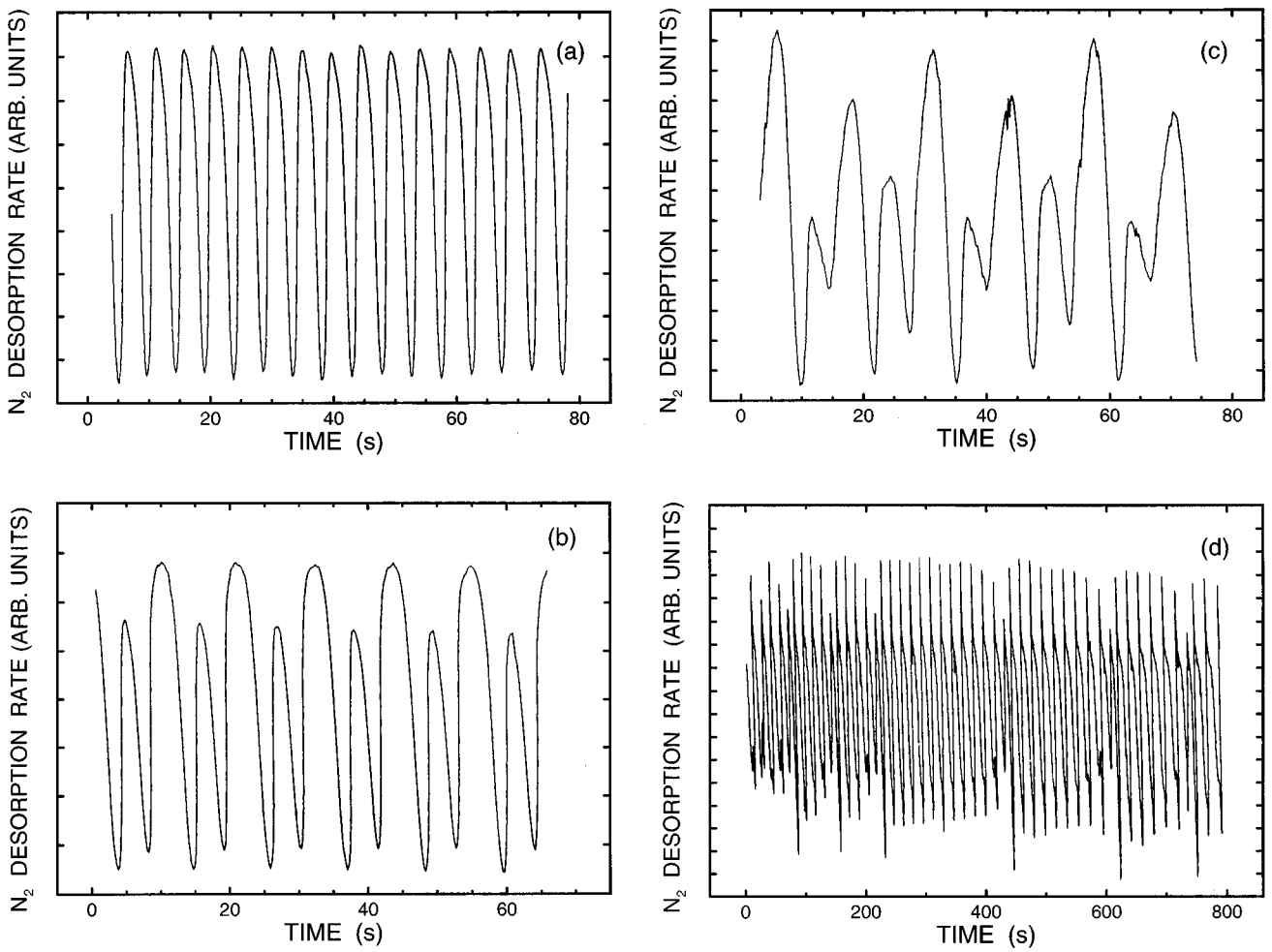

FIG. 18. Rate of N_2 desorption as a function of time during the NO-H_2 reaction on Pt(100) at $P_{NO}=3\times10^{-9}$ bar and $T=460$ K. (a) Period-1 oscillations at $P_{NO}/P_{H_2}=1$, (b) period-2, (c) period-4, and (d) aperiodic oscillations at $P_{NO}/P_{H_2}\simeq1.4$ (redrawn from Ref. [14]).

reason, it was of interest to study the reaction kinetics at higher diffusion rates. Our experience indicates that further increase of the NO diffusion rate does not change qualitatively the results. To illustrate the latter conclusion, we show in Figs. 16 and 17 the oscillatory kinetics and lattice snapshots calculated for $p_{NO}=0.03$ with $N_{dif}=10\,000$. With increasing N_{dif} from 1000 to 10 000, the amplitude of oscillations becomes larger but only a little (Fig. 16). The size of islands increases as well [cf. Figs. 3(b) and 17] but not dramatically.

We have also proven that the kinetics calculated are stable with respect to variation of L. For varying L from 100 to 400, the amplitude of oscillations decreases but only slightly. Thus, adsorbate diffusion is able, in our case, to maintain synchronization of oscillations. For very large lattices ($L\gg500$), this mechanism synchronization may in principle be weak at very long times (for a discussion, see Ref. [5]). Nevertheless, the oscillations can really be observed provided that the desynchronization time is longer compared to the time of measurements. Alternatively, synchronization of oscillations might occur via the gas phase (detailed discussion of the latter phenomenon is beyond our goals).

VII. SIMULATIONS VS EXPERIMENT

The main goal of our simulations was to show the type of oscillations and spatiotemporal patterns predicted by the model. A full-scale analysis of oscillations observed experimentally [13–15] in the system under consideration is beyond the scope of our study. Without comparing experiment and simulations, the presentation would, however, not be complete. Bearing in mind this point, we show in Fig. 18 typical experimental data [14] exhibiting the transition from period-1 oscillations to aperiodic oscillations. The governing parameter in the experiment is P_{NO}/P_{H_2}. Physically, this parameter is close to that, p_{NO}, used in our simulations. Thus, it makes sense to compare the evolution of oscillations observed with increasing value of the governing parameter in the experiment and simulations. In both cases, we have first almost harmonic oscillations [cf. Figs. 6(a) and 18(a)], then period-2 oscillations [cf. Figs. 9(a) and 18(b)], then period-2 or period-4 oscillations with very similar shape [cf. Figs. 10(a) and 18(c)], and finally irregular oscillations [cf. Figs. 13(a) and 18(d)]. Thus, the reaction kinetics observed in the experiment and simulations are in good qualitative agreement.

VIII. CONCLUSION

We have presented comprehensive Monte Carlo simulations of kinetic oscillations in the NO-H_2 reaction on the Pt(100) surface in the framework of the lattice-gas model explicitly describing adsorbate-induced surface restructuring

in terms of the theory of first-order phase transitions. On the nm scale, the model predicts formation of restructured islands with atomically sharp boundaries. The shape of islands is strongly dependent on the reaction conditions. Despite phase separation on the surface, the transition from almost harmonic oscillations to chaos is found to occur via the standard Feigenbaum scenario. Near the critical point, the dependence of the amplitude of oscillations on the governing parameter is shown to be close to that predicted for the Hopf supercritical bifurcation.

The statistical model employed in our study is rather general. It makes it possible to simulate different aspects of the kinetics of catalytic reactions accompanied by adsorbate-induced surface restructuring by changing values of lateral interaction and rules for elementary processes.

ACKNOWLEDGMENT

The author thanks B. Kasemo for useful discussions.

[1] R. Imbihl and G. Ertl, Chem. Rev. **95**, 697 (1995).
[2] M. Gruyters and D.A. King, J. Chem. Soc., Faraday Trans. **93**, 2947 (1997).
[3] G. Ertl, P.R. Norton, and J. Rüstig, Phys. Rev. Lett. **49**, 177 (1982).
[4] R. Danielak, A. Perera, M. Moreau, M. Frankowicz, and R. Kapral, Physica A **229**, 428 (1996); V.N. Kuzovkov, O. Kortlüke, and W. von Niessen, J. Chem. Phys. **108**, 5571 (1998); E.V. Albano, *ibid.* **109**, 7498 (1998).
[5] R.J. Gelten, A.P. Jansen, R.A. van Santen, J.J. Lukkien, J.P.L. Sergers, and P.A.J. Hibers, J. Chem. Phys. **108**, 5921 (1998), and references therein.
[6] T.E. Jackman, K. Griffith, J.A. Davies, and P.R. Norton, J. Chem. Phys. **79**, 3529 (1983).
[7] M. Kim, W.S. Sim, and D.A. King, J. Chem. Soc., Faraday Trans. **92**, 4781 (1996).
[8] V. Gorodetskii, J. Lauterbach, H.H. Rotermund, J.H. Block, and G. Ertl, Nature (London) **370**, 276 (1994).
[9] Yu. Suchorski, J. Beben, and R. Imbihl, Surf. Sci. **405**, L477 (1998).
[10] V.P. Zhdanov and B. Kasemo, J. Stat. Phys. **90**, 79 (1998).
[11] V.P. Zhdanov, J. Chem. Phys. **110**, 8748 (1999); Surf. Sci. (to be published).
[12] V.P. Zhdanov and B. Kasemo, Appl. Catal., A (to be published).
[13] J. Siera, P. Cobden, K. Tanaka, and B.E. Nieuwenhuys, Catal. Lett. **10**, 335 (1991).
[14] P. Cobden, J. Siera, K. Tanaka, and B.E. Nieuwenhuys, J. Vac. Sci. Technol. A **10**, 2487 (1992).
[15] M. Slinko, T. Fink, T. Löher, H.H. Madden, S.J. Lombardo, R. Imbihl, and G. Ertl, Surf. Sci. **264**, 157 (1992); **269**, 481 (1992).
[16] S.J. Lombardo, T. Fink, and R. Imbihl, J. Chem. Phys. **98**, 5526 (1993).
[17] M. Gruyters, A.T. Pasteur, and D.A. King, J. Chem. Soc., Faraday Trans. **92**, 2941 (1996).
[18] A.G. Makeev and B.E. Nieuwenhuys, (a) J. Chem. Phys. **108**, 3740 (1998); (b) Surf. Sci. **418**, 432 (1998).
[19] B. Hellsing, B. Kasemo, and V.P. Zhdanov, J. Catal. **132**, 210 (1991).
[20] V.P. Zhdanov, *Elementary Physicochemical Processes on Solid Surfaces* (Plenum, New York, 1991).
[21] V.P. Zhdanov and B. Kasemo, J. Chem. Phys. **104**, 2446 (1996).
[22] S.K. Scott, *Chemical Chaos* (Clarendon Press, Oxford, 1991).